HHS Public Access

Author manuscript

J Alzheimers Dis. Author manuscript; available in PMC 2018 May 04.

Published in final edited form as:

J Alzheimers Dis. 2017 ; 59(1): 223–239. doi:10.3233/JAD-170283.

Mitochondrial Dysfunction Triggers Synaptic Deficits via Activation of p38 MAP Kinase Signaling in Differentiated Alzheimer's Disease Trans-Mitochondrial Cybrid Cells

Qing Yu[$,a,1], **Fang Du**[a,1], **Justin T. Douglas**[#], **Haiyang Yu**[$,*], **Shirley ShiDu Yan**[a], and **Shi Fang Yan**[a,*]

[$]State Key Laboratory of Oral Diseases, National Clinical Research Center for Oral Diseases, West China Hospital of Stomatology, Sichuan University, Cheng Du, China

[a]Departments of Pharmacology and Toxicology, and Higuchi Bioscience Center, University of Kansas, Lawrence, KS, USA

[#]Nuclear Magnetic Resonance Laboratory, Molecular Structures group, University of Kansas, Lawrence, KS, USA

Abstract

Loss of synapse and synaptic dysfunction contribute importantly to cognitive impairment in Alzheimer's disease (AD). Mitochondrial dysfunction and oxidative stress are early pathological features in AD-affected brain. However, the effect of AD mitochondria on synaptogenesis remains to be determined. Using human transmitochondrial "cybrid" (cytoplasmic hybrid) neuronal cells whose mitochondria were transferred from platelets of patients with sporadic AD or age-matched non-AD subjects with relatively normal cognition, we provide the first evidence of mitochondrial dysfunction compromises synaptic development and formation of synapse in AD cybrid cells in response to chemical-induced neuronal differentiation. Compared to non-AD control cybrids, AD cybrid cells showed synaptic loss which was evidenced by a significant reduction in expression of two synaptic marker proteins: synaptophysin (presynaptic marker) and postsynaptic density protein-95, and neuronal proteins (MAP-2 and NeuN) upon neuronal differentiation. In parallel, AD-mediated synaptic deficits correlate to mitochondrial dysfunction and oxidative stress as well as activation of p38 MAP kinase. Notably, inhibition of p38 MAP kinase by pharmacological specific p38 inhibitor significantly increased synaptic density, improved mitochondrial function, and reduced oxidative stress. These results suggest that activation of p38 MAP kinase signaling pathway contributes to AD-mediated impairment in neurogenesis, possibly by inhibiting the neuronal differentiation. Our results provide new insight into the crosstalk of dysfunctional AD mitochondria to synaptic formation and maturation *via* activation of p38 MAP kinase. Therefore, blockade of p38 MAP kinase signal transduction could be a potential therapeutic strategy for AD by alleviating loss of synapses.

[*]Correspondence to: Shi Fang Yan, MD, Higuchi Bioscience Center, University of Kansas, 2099 Constant Avenue, Lawrence, KS 66047, USA. Tel.: +1 785 864 1987; sfangyan@ku.edu and Haiyang Yu, MD, State Key Laboratory of Oral Diseases, National Clinical Research Center for Oral Diseases, West China Hospital of Stomatology, Sichuan University, Cheng Du, 610041, China.

[1]These authors contributed equally to this work.

SUPPLEMENTARY MATERIAL

The supplementary material is available in the electronic version of this article: http://dx.doi.org/10.3233/JAD-170283.

Keywords

Alzheimer's disease; cybrid cells; mitochondrial dysfunction; synaptic deficits

INTRODUCTION

Alzheimer's disease (AD) is a progressive neurodegenerative disorder and begins with a prominent impairment in cognitive function. At the early stage, patients with this devastating disease exhibit an inability to encode new memories of events or facts. Intact synaptic structure and function are essential for the synaptic encoding that forms stable memories [1, 2]. While the molecular basis for early onset of AD is elusive [3], the structural and functional deficits in synapses are highly correlated with memory and cognitive impairment [4–7]. Given that synapse loss appears to be a morphological reflection of the synaptic dysfunction that begins earlier than amyloid-β (Aβ) plaque formation and neuronal loss [8], synaptic deficiency has been considered to be an early sign of AD [9–11]. Loss of pre-synaptic or post-synaptic proteins, such as synaptophysin (presynaptic protein) [12] or postsynaptic density protein-95 (PSD95) [9], were demonstrated in early stage of AD transgenic mice and AD patients.

Mitochondrial dysfunction is well-known to associate with AD progression [13]. Aβ progressively accumulates in mitochondria and is associated with diminished enzymatic activity of respiratory chain complexes and a reduction in the rate of oxygen consumption [14, 15]. Cytoplasmic hybrid ("cybrid") technology, with the transfer of mitochondria from affected patients to cell lines deficient in mitochondria (Rho^0 cells), have been used to investigate the role of dysfunctional mitochondria in AD pathogenesis [16–18]. These human AD cybrid neuronal lines recapitulate mitochondrial structural and functional changes observed in AD-affected brains. AD cybrids reveal a decrease in cytochrome c oxidase, a key enzyme of respiratory chain, increased free radical production, impaired intracellular calcium buffering, fission-fusion imbalance, and decreased mitochondrial energy metabolism [17, 19–21]. Although AD cybrid cells can differentiate into a mature neuronal phenotype with the appearance of neuronal processes in the presence of staurosporine, 12-O-tetradecanoyl phorbol-13 acetate, their neuronal processes are shorter and less density as compared to non-AD differentiated cells [22]. Furthermore, differentiated AD cybrids exhibited mitochondrial defects, including disruption of mitochondrial respiration, aberrant energy metabolism, and significant reduction in mitochondrial transport, which was accompanied by increased mitochondrial oxidative stress. These are resembling characteristics of AD. It is unclear why and how neurons containing AD-derived mitochondria suffer synaptic pathology and a link of aberrant AD mitochondria to synaptic alteration remains to be determined.

AD transmitochondrial cytoplasmic hybrid (cybrid) neuronal cell lines with incorporated platelet mitochondria from sporadic AD or cognitively normal age-matched subjects [17, 22–24] were used to model human AD-relevant mitochondrial function. We comprehensively evaluated the effect of mitochondrial dysfunction on synaptic development during the neuronal differentiation to address whether dysfunctional AD mitochondria

disturbs synaptogenesis and whether oxidative stress-mediated activation signaling potentiates the development of synapses, which links to mitochondrial abnormalities. Our results demonstrate that AD-affected mitochondria elicited detrimental effects on synaptic development *via* activation of p38 MAP kinase signaling pathway in AD cybrid cells. Inhibition of p38 MAP kinase activation blocked these detrimental effects. These studies explore a pivotal role of p38 MAP kinase pathway in mediating mitochondrial dysfunction and synaptic deficits in AD pathogenesis.

MATERIALS AND METHODS

Human subjects and creation of cybrid cell lines

Both AD patients and non-AD controls were recruited from the University of Kansas Alzheimer's Disease Center (KUADC). Subjects with AD met the National Institute of Neurological and Communicative Disorders and Stroke and the Alzheimer's Disease and Related Disorders Association criteria [25]. This study was approved by the University of Kansas Medical Center (KUMC) Institutional Review Board. Non-AD subjects were cognitively normal and age-matched to AD subjects. All subjects provided written informed consent to participate in the study. The ages of AD and non-AD platelet donors were 73.6 ± 2.96 and 75.8 ± 5.04 years, respectively. The detailed information about gender, age, and disease status of donors is presented in Supplementary Table 1. All AD cases are sporadic and not due to APP/PS1/PS2 mutations, which do not show a clear Mendelian inheritance pattern, are essentially considered sporadic (i.e. they are not recognizably autosomal recessive or dominant). The mutation cases are incredibly rare, probably around 500 families in the world. Age of onset is usually in the 40 s or 50 s. They account for well less than 1% of AD cases. As long as a patient is >60 years old and does not have a parent who also developed AD before the age of 60, the chances of someone being Mendelian (rather than sporadic) is incredibly low. We do not have interest in making cybrids from mutation subjects because presumably the mitochondrial defects would be corrected in cell culture, since the mitochondria are separated from the presence of the nuclear mutation when we do the transfection into the Rho^0 cells.

Cybrid cell lines were created on the human neuroblastoma cell (SH-SY5Y) nuclear background (by the KU ADC Mitochondrial Genomics and Metabolism Core) [26]. There are several reasons to select SH-SY5Y cells to create AD cybrid cells: 1) They are a commonly used human neuronal line and available in the laboratory when we decided to generate human neuronal cybrid cell line and 2) they can be differentiated into neuronal-like cells. Importantly, SH-SY5Y cells has been very successfully transmitted by mitochondria derived from human AD and non-AD subject as a human AD cybrid cell lines that recapitulate specific AD mitochondriopathies [17, 18, 22, 24, 27]. To create the cybrid cell lines used for this study, SH-SY5Y cells that were previously depleted of endogenous mtDNA (Rho^0 cells), which were fused with platelet cytoplasm from human subjects, and repopulated with mitochondria containing mtDNA from patients or controls as previously described [28]. The quantitative real-time PCR showed that the intact mtDNA copies were present in all cybrids without detectable large scale deletion after many passages of cell proliferation as previously described [22].

Cybrid growth and differentiation

AD and non-AD cybrid cells were grown in T75 tissue culture flasks in Dulbecco's modified Eagle's medium (DMEM) supplemented with 10% characterized fetal bovine serum (FBS; Gibco BRL, Logan, Utah), 100 μg/ml pyruvate, 50 μg/ml uridine, antibiotic-antimycotic,100 Units/ml penicillin G, and 100 μg/ml streptomycin as previously described [17]. Culture media were replaced to the differentiation media [neurobasal media supplemented with 1× B27 (Invitrogen, Carlsbad, CA) and 0.5 mM glutamine, and antibiotic-antimycotic] with 10 nM staurosporine (SAT, Sigma-Aldrich Corp, St. Louis, Missouri, USA). Half of the differentiation media were made fresh with 10 nM SAT and replaced every day as previously described [22]. To assess the effects of the inhibitor of p38 on cybrid cells, 1 μM SB203580 (EMD Chemicals, Inc.) were added to the media 30 min before replaced by differentiation media and also keep the SB203580 along with the differentiation. Based on the measurement of length of neuronal processes, day-14 cybrid cells reached plateau after differentiation in day-35 (data not shown), indicating that differentiation was completed on day 14 after SAT treatment.

Immunocytochemistry

Undifferentiated and differentiated cybrid cells cultured on coverslips, which were fixed in 4% paraformaldehyde, and then permeability with 0.1%Triton X-100 in PBS. Cells were incubated in blocking solution (5% goat serum in PBS) for 20 min and then incubated with different primary antibodies: mouse anti-MAP2 (1:2000, #1284959, Chemicon), rabbit anti-NeuN (1:1000, #ABN78, Chemicon), rabbit Anti-Synaptophysin (1:5000, #AB9272, Millipore), and mouse anti-PSD95 antibody (1:1000, #P246, Sigma), respectively, overnight at 4°C. After washing three times with PBS, cells were incubated with Alexa Fluor® 594 conjugated goat anti-rabbit IgG or 488 goat anti-mouse IgG secondary antibodies at 1:1000 dilutions for 2 h at room temperature. Fluorescence images were acquired using a Leica SP5 confocal microscope and were analyzed with Leica LAS AF software (Leica Wetzlar).

Western blot analysis

Samples were lysed in extraction buffer [10 mM Tris-HCl (pH 7.4), 100 mM sodium chloride, 1 mM EDTA, 1 mM EGTA, 1 mM sodium fluoride, 20 mM sodium pyrophosphate, 2 mM sodium orthovanadate, 1% Triton X-100, 10% glycerol, 0.1% SDS, 0.5% deoxycholate, 1 mM PMSF] containing protease inhibitor mixture (set V, EDTA-free; Calbiochem, San Diego, CA), separated by SDS/PAGE (12% Bis-Tris gel; Invitrogen), and then transferred to a nitrocellulose membrane (Amersham, Pittsburgh, PA). After blocking in TBST buffer (20 mM Tris-HCl, 150 mM sodium chloride, 0.1% Tween-20) containing 5% (wt/vol) nonfat dry milk (Santa Cruz) for 1 h at room temperature, the membrane was then incubated and gently shaken overnight (at 4°C) with a primary antibody. The primary antibodies were mouse anti-MAP2 (1:2000, #1284959, Chemicon), rabbit anti-NeuN (1:1000, #ABN78, Chemicon), rabbit anti-synaptophysin (syn, 1:5000, #AB9272, Millipore), mouse anti-PSD95 antibody (1:1000, # P246, Sigma), anti-phos-p38 (1:1000, #612288, BD), anti-total-p38 (1:1000, #9212, Cell signaling). The membranes were incubated for 2 h with horseradish (HRP)-conjugated secondary antibodies (SIGMA, USA) after washing with TBST three times. Final detection of immunoreactive bands was

performed by using enhanced chemiluminescence (Pierce™ ECL Western Blotting Substrate, Thermo Fisher, USA). Anti-mouse β-actin monoclonal antibody (Sigma-Aldrich, MO) at a 1:10,000 dilution was used to ensure equal protein loading of the samples.

Measurement of respiratory chain complexes enzyme activities and ATP levels

Enzyme complex IV (cytochrome c oxidase) activity, and ATP levels were determined as described previously [17]. Briefly, cybrid cells were washed with ice-cold PBS, and then harvested, centrifuged, and suspended in 50 μl of isolation buffer containing 250 mM sucrose, 20 mM HEPES, and 1 mM EDTA. Cell suspensions (containing ~3–4 mg of protein/ml) were added to a cuvette containing 0.95 ml of 1× assay buffer (10 mM Tris-HCl, and 120 mM KCl), and the reaction volume was brought to 1.05 ml with the addition of 1× enzyme dilution buffer (10 mM Tris-HCl, pH 7.0). The reaction was then initiated by the addition of 50 μl of ferrocytochrome substrate solution (0.22 mM). The rate of change in absorbance at 550 nm was recorded immediately using a Shimadzu (Kyoto, Japan) UV1200 spectrophotometer programed for a 5-s delay and 10-s intervals for 6 readings. Data of cytochrome c oxidase activity are expressed as micromoles of cytochrome oxidized per min $^{-1}$ mg^{-1} protein using an extinction coefficient of 18.64 mM^{-1} cm^{-1}. ATP levels were determined using an ATP Bioluminescence Assay Kit (Roche) following the manufacturer's instruction as we previously described [29, 30]. Briefly, cells were quickly harvested by ATP lysis buffer, incubated on ice for 30 min, and then centrifuged at 12,000 g for 10 min. ATP levels were measured using a Luminescence plate reader (Molecular Devices). A 1.6-s delay time after substrate injection and 10 s integration time were used.

Evaluation of mitochondrial and intracellular reactive oxygen species (ROS)

Cybrid cells were seeded at low density onto Lab-Tek eight-well chamber slides (10000 cells/well). Mitochondrial ROS generation was determined using MitoSox Red (Invitrogen), a unique fluorogenic dye highly selective for detection of superoxide production in live cell mitochondria. Cells were incubated with fresh medium containing 2.5 μM MitoSox for 30 min. Fluorescence images were acquired using a Leica SP5 confocal microscope and analyzed using Leica LAS AF software (Leica Wetzlar). Excitation wavelengths were 543 nm for MitoSox, and fluorescent signals were quantified using NIH Image J software.

Evaluation of intracellular ROS levels was assessed by election paramagnetic resonance (EPR) spectroscopy as described in our previous study [14, 31]. Cybrid cells cultured on 6-well plates were washed with PBS and then incubated with CMH (Cyclic hydroxylamine 1-hydroxy-3-methoxycarbonyl-2, 2, 5, 5-tetramethyl-pyrrolidine, 100 μM) at room temperature for 30 min. After that, cybrid cells were washed with ice-cold PBS, and then harvested with 100 μl of PBS for each well. EPR measurements were performed using a Bruker EMX plus X-band EPR spectrometer running Bruker Xenon acquisition/processing software and equipped with a dual mode cavity (ER4116DM) and Oxford ESR900 cryostat. For each sample ~50 μl was loaded into a 1.5 mm O.D. micropipette (Blaubrand intraMARK), sealed with Bruker X-Sealant and placed into a 4 mm O.D. EPR tube (Wilmad Labglass 707-SQ-250M). The EPR spectrometer was operated at 9.63 GHz and 100 kHz field modulation at room temperature. The spectra were recorded with the following parameters: number of scans, 3; magnetic field center, 344 mT; scan range, 10 mT;

microwave power, 2 mW; modulation amplitude, and 0.1 mT; time constant, 0.08 s. Signal intensity was determined as the height of the central peak on the up-field side of the midpoint.

Determination of mitochondrial membrane potential (ΔΨ) with TMRM

To detect mitochondrial membrane potential, cells were co-stained with TMRM (100 nM; Invitrogen) for 30 min. Mitochondria were labeled with Mito-tracker Red (MTRed, 100 nM, Invitrogen) and/or MitoTracker Green without interference of mitochondrial membrane potential (MTGreen, 100 nM, Invitrogen) for 30 min at 37°C before fixation to visualize mitochondrial morphology. To validate the specificity of TMRM dye, 10 μm carbonyl cyanide 4-(trifluoromethoxy) phenylhydrazone (FCCP) to collapse ΔΨ, and the obtained TMRM fluorescence was used to set the threshold.

Fluorescence images were acquired using a Leica SP5 confocal microscope and analyzed using Leica LAS AF software (Leica Wetzlar). Excitation wavelengths were 543 nm for TMRM or MTRed, and 488 nm for MTGreen, respectively. NIH Image J software for quantification of fluorescent signals and measurement of mitochondrial density.

Statistical analysis

Data are presented as mean ± SEM. Statistical analysis was performed using Statview software (SAS Institute, Version 5.0.1). Differences between means were assessed by one-way analysis of variance (ANOVA) with Fisher posthoc test. $p < 0.05$ was considered significant.

RESULTS

Differentiation of AD and non-AD cybrid cells

Morphological changes were observed in non-AD (Fig. 1A II) and AD cybrid cells (Fig. 1A IV) treated with staurosporine (SAT) under serum free conditions. SAT, a chemical stimulus, serves as a particularly strong inducer of differentiation in the SH-SY5Y cells. The concentration of SAT between 4 and 25 nM has been used in a wide range of cells without toxic effect [32–34]. As such, we treated cybrid cells with 10 nM SAT for 14 days. Differentiated cells began to appear 3 days after SAT treatment and differentiation was complete on day 14. Over the course of a month, no cell detachment or apoptosis (based on stains to detect apoptosis) was observed. In the presence of 10 nM SAT for 14 days, a typical differentiated morphology was visualized as long and straight neuronal-like processes stretched out in the non-AD cybrid cells (Fig. 1A II). In contrast, differentiated AD cells revealed much shorter neuronal like processes than differentiated non-AD cells (Fig. 1A IV). Neuronal process length showed an almost 3-fold increase in differentiated non-AD cybrid cells compared to undifferentiated non-AD cells, whereas only a slight increase by 1.3-fold in the processes was observed in the differentiated AD cybrid cells compared to undifferentiated AD cybrid cells (Fig. 1B). There were no statistically significant difference in process length between the undifferentiated non-AD and AD cybrid cells; however, compared to differentiated non-AD cybrid cells, differentiated AD cybrid cells revealed

shorter neuronal-like processes, suggesting the impairment in the differentiation capacity of cybrid cells containing AD-derived mitochondria.

To further compare the difference between non-AD and AD cybrid cells in differentiation, we investigated the expression levels of neuronal markers in both cells with or without SAT treatment by immunoblotting and immunohistochemistry analyses. Microtubule-associated protein 2 (MAP2), a neuron-specific protein that stabilizes microtubules in the dendrites of postmitotic neurons, is widely used as a marker of neuronal differentiation [35]. Neuronal nuclear antigen (NeuN) appears highly specific as a marker of neuronal nuclei, also a marker of neuronal maturation [36]. Immunoblotting of cell lysates showed that MAP2 or NeuN levels were robustly elevated by ~10- or ~26-fold in differentiated non-AD cybrid cells compared to undifferentiated non-AD cells (Fig. 2A, B), suggesting a good capacity of differentiation in non-AD cybrid cells. However, MAP2 or NeuN levels were only increased by ~5- or ~12-fold in differentiated AD cybrid cells compared to undifferentiated AD cybrid cells, suggesting the impairment in the differentiation of AD-derived mitochondria. Consistent with immunoblotting results, immunoreactivity of MAP2 or NeuN was present in both differentiated non-AD and AD cybrid cells (Fig. 2E). There were significant reduced levels of MAP2 or NeuN immunoreactivity in differentiated AD cybrid cells compared to differentiated non-AD cybrid cells (4.6- versus 27-fold for MAP2 and 2.4-versus 5-fold for NeuN) (Fig. 2C–E). Overall, levels of MAP2 or NeuN in differentiated AD cybrid cells was significantly lower than that observed in differentiated non-AD cybrid cells. These data suggest that AD and non-AD cybrid cells have the capacity to differentiate neuronal like cells with axon-like neuronal process morphology. However, AD cybrid cells reveal the impairment in their capacity of differentiation into the neuronal like properties.

We next examined the effect of AD-derived mitochondria on synaptic protein expression and neuronal formation in AD cybrid cells compared to non-AD cybrid cells undergoing differentiation. The proper expression levels of the pre- and post-synaptic proteins, including synaptophysin and PSD95, were essential components for structure and function of synapses [37]. The differentiated non-AD cybrid cells induced by SAT demonstrated a robust increase in intensity of immunoreactive band for synaptophysin or PSD95 by 11- or 25-fold compared to undfferentiated non-AD cells (Fig. 3A). However, synaptophysin or PSD95 levels were only increased by 1.5- or 3-fold in the differentiated AD cybrid cells in comparison with undfferentiated AD cybrid cells (Fig. 3A). Similarly, immunoreactivity of synaptophysin (red) or PSD95 (green) appeared in the differentiated non-AD and AD cybid cells with different fluorescence intensity. (Fig. 3D). Quantification of the intensity of immunofluorescence demonstrated significant increases in the fluorescence intensity of synaptophysin (Fig. 3B) and PSD95 (Fig. 3C) in differentiated non-AD and AD cybrid cells compared to either the undifferentiated non-AD cybrid cells ($p < 0.01$) or the AD cybrid cells ($p < 0.01$). Clearly, fluorescence intensity of synaptophysin or PSD95 was strikingly reduced by 5–6 fold in the differentiated AD cybrid cells compared to the differentiated non-AD cells. In the representative immunostaining images, either synaptophysin or PSD95 were clearly visualized and evenly distributed along the differentiated processes of non-AD and AD cybrid cells, whereas both synaptic proteins were dramatically reduced in AD cybrid cells compared to non-AD cybrid cells upon differentiation (Fig. 3D). Accordingly, AD cybrids cells exhibit synaptic deficits evidenced by lower expression of synaptophysin and

PSD95, thus, impaired their ability to assembly full process lengths during neuronal-like differentiation.

Effect of p38 inhibitor on neuronal-like differentiation and development of synapses in AD cybrid cells

In view of significance on the activation of p38 MAP kinase in AD mitochondrial and synaptic alterations [24, 38, 39], we first assessed levels of the phosphorylation of p38 MAP kinase in this *in vitro* human cell upon differentiation by immunoblotting. The phosphorylation of p38 was robustly increased in AD cybrid cells compared to non-AD cybrid cells. Notably, treatment with a specific inhibitor of p38 (SB203580 1 μM) abolished p38 phosphorylation in AD cybrid cells compared to vehicle treatment. Similar blocking effect of p38 inhibitor was observed in non-AD cybrid cells (Fig. 4A). No significant change in total p38 was found in AD cybrid cells. Given that activation of p38 MAP kinase signaling pathway in AD-derived mitochondria might contribute to defective neuronal differentiation and synaptic structure and function, we sought to examine whether inhibition of p38 signaling pathway could ameliorate the pathologic events relevant to neuronal maturation in AD cybrid cells. AD cybrid cells were incubated with an inhibitor of p38, SB203580 1 μM, and then evaluated for neuronal morphology and synaptic protein expression in the presence of SAT to induce cell differentiation. In the presence of p38 inhibitor, AD cybrid cells revealed significantly increased neuronal-like processes and length of processes (Fig. 4B, C) compared to vehicle-treated AD cells under normal differentiation condition with SAT. Accordingly, loss of neuronal markers for MAP2 and NeuN were completely restored in differentiated AD cybrid cells in the presence of SB203580 compared to the absence of SB203580 (Fig. 4D), in parallel, the expression of pre- and post-synaptic proteins, synaptophysin and PSD95, were also rescued in differentiated AD cybrid cells exposed to SB203580 compared with vehicle control cells (Fig. 4E). These results indicate the protective effect of blocking p38 activation on deficit in neuronal differentiation and synaptic formation insulted by AD mitochondria.

Effect of p38 inhibitor on mitochondrial oxidative stress and function

Given that oxidative stress is important for the activation of p38 MAP kinase and that mitochondria are a major source of ROS production, we next to determine a connection of mitochondrial oxidative stress to activation of p38 signals in AD-derived mitochondria. We first examined the effect of p38 on mitochondrial oxidative stress by determining mitochondria-derived ROS. Consistent with our previous observation, differentiated AD cybrid cells demonstrated a significantly increased ROS [22] compared to non-AD cybrid cells. MitoSox-Red signals, an indicator of mitochondrial superoxide, were greatly increased in differentiated AD cybrid cells in comparison with non-AD cybrid cells (Fig. 5A, B), suggesting increased levels of mitochondrial ROS in AD cybrid cells [22]. Treatment of p38 inhibitor completely eliminated excessive MitoSox signals. There was no effect of p38 inhibitor in non-AD cybrid cells compared to vehicle-treated control cells, suggesting nontoxic effect of p38 inhibitor SB203580 on cells. Furthermore, we quantitatively measured the intracellular ROS levels in the cells by highly sensitive and specific EPR spectroscopy. The intracellular ROS levels indicated by EPR peaks were significantly elevated in differentiated AD cybrid cells compared to non-AD cells. This was robustly

blocked by the addition of p38 inhibitor SB203580. These results suggest that blocking the activation of p38 MAP kinase reduces mitochondrial oxidative stress in AD-affected mitochondria.

Next, we evaluated mitochondrial function by examining mitochondrial respiratory chain activity, membrane potential, and ATP level. In response to SAT-induced differentiation, AD cybrid cells revealed decreases in cytochrome c oxidase activity, a key enzyme of complex IV in the respiratory chain, ATP levels, and TMRM as an indicator of mitochondrial membrane potential compared to non-AD cybrid cells. The addition of FCCP, an uncoupling mitochondrial membrane agent, abolished TMRM signals (Fig. 5H), indicating the specific reaction of TMRM as an indicator of mitochondrial membrane potential. Notably, treatment of p38 inhibitor SB203580 alleviated these detrimental effects in differentiated AD cybrid cells as shown by increased complex IV activity, ATP levels (Fig. 5E, F) and mitochondrial membrane potential (Fig. 5G, H). These data suggest that the inhibition of p38 MAP kinase activation ameliorates AD-specific mitochondrial dysfunction in the differentiated AD cybrid cells.

DISCUSSION

Oxidative stress, mitochondrial dysfunction, and synaptic loss are early features in the pathogenesis of AD. Abnormal mitochondrial permeability transition pore [29] and impairment in mitochondrial clearance such as inactivation of mitochondrial degrading enzyme cause accumulation of mitochondrial Aβ and potentiate aberrant mitochondria [14, 40]. Interaction of Aβ with mitochondrial protein enhances ROS production and accumulation, which in turn triggers opening of mPTP and release mitochondrial protein (cytochrome C) to cytosol, leading to the activation of signal transduction such as p38 MAP kinase and apoptosis [15, 41–43]. In this study, we illustrated that AD-affected mitochondria act as a trigger for increasing levels of ROS, subsequently, elevated ROS promotes activation of p38 MAP kinase signaling pathway. One after another, the activated p38 MAP kinase critically contributes to neuronal differentiation impairment and synaptic deficits in AD cybrid cells via augmentation of mitochondrial oxidative stress and consequent amplification of mitochondrial dysfunction. Blockade of p38 MAP kinase signaling in AD cybrids by a pharmacological p38 inhibitor ameliorated AD-associated detrimental impacts aforementioned. Our findings highlighted a pivotal role of p38 MAP kinase signaling in mediating mitochondrial dysfunction and synaptogenesis in pathogenesis of AD (Fig. 6).

It has been demonstrated that ROS and phosphorylated p38 MAP kinase are significantly elevated in undifferentiated and differentiated AD cybrid cells compared to non-AD cybrids [17, 22, 24]. Activation of p38 MAP kinase is associated with increased ROS production/accumulation and mitochondrial stress [39, 44–46] and contributes to synaptic dysfunction [47–49]. The antioxidant blocked p38 activation along with attenuating mitochondrial perturbation. Furthermore, the suppression of the p38 MAP kinase pathway also results in a prevention of oxidative stress-induced mitochondrial and cellular perturbation [39, 50]. Thus, increases in ROS generation in AD cybrid cells containing AD mitochondria could trigger activation of p38 MAP kinase signaling, which in turn exacerbate mitochondrial and neuronal dysfunction. Indeed, the suppression of ROS rescues mitochondrial function,

transport, and mitochondrial dynamics [17, 22]. Given the link of ROS to synaptic mitochondrial and synaptic alterations and the vital role of synaptic mitochondria in synaptic transmission [14, 22, 29, 30, 39, 51–55], we propose that AD-associated ROS production could directly or indirectly affect cell differentiation as shown by compromised synaptic development and formation of synapse in AD-derived mitochondria in response to chemical-induced neuronal differentiation. Inhibition of excessive ROS and activation of p38 MAP kinase rescues impairment in synaptic development and formation of synapses as shown by increased expression levels of pre- and post-synaptic proteins.

The differentiation capacity of cybrid cells was noted and compared by measuring the expressions of neuronal markers such as MAP2 and NeuN. Previous studies have shown increased expressions of neuronal markers in neuronal SH-SY5Y cells under differentiation [56, 57]. It was report that staurosporine is capable of inducing apoptosis or cellular perturbation in neuron cells including SH-SY5 [58, 59], AF5 neural cells derived fetal rat mesencephalic tissue [60], rat hippocampus neurons [61], and human cortical neurons (HCN-1A) [62]. However, the concentration of staurosporine used for the experiments ranges from 250 nM to 10 μM, which is significantly higher than what we used in our differentiation system (10 nM). It is almost 25–1000 times higher than the concentration in our culture with staurosporine treatment in order to induce cellular dysfunction or apoptosis. MAP2 is an abundant neuronal cytoskeletal protein regulating the structure and stability of microtubules, and it is also employed as a marker for neuronal maturation [63]. We found that MAP2 levels were markedly increased in the differentiated non-AD cybrid cells, from their cell bodies to processes, in comparison with their undifferentiated status. Although the increase could be detected in the cellular bodies in the AD cybrid cells with SAT treatment, the elevation of these two neuronal proteins was insignificant in the impaired processes, indicating an ill-differentiation in the processes of AD cells. Consistent with our data, the numbers of MAP2 immunoreactive neurons were reported ~30% less in AβPP transgenic mice than nontransgenic mice at 2–3 months of age, well before Aβ plaque formation [64]. In addition, another marker of neuronal maturation, NeuN, which is present in nuclei of most neuronal cells throughout the nervous system of adult brain [65], increased expression could be found in the nuclei of both differentiated non-AD and AD cybrid cells compared with the levels of their undifferential status. However, a significant difference could be found between the differentiated non-AD and AD cells, suggesting that AD cybrids in differentiation was less matured than the non-AD cells, though AD cells could be induced to matured cell body with SAT treatment. The changes in the neuronal markers demonstrated that AD cybrids are less matured under differentiation, especially in the processes, where the AD cells have impaired expression of the neuronal markers. There are many other proteins, which have been found in the synapse that change their expression during the development and disease state, including proteins related to synaptic vesicle postsynaptic density and presynaptic active zone. Oxidative stress potentiates synaptic alterations relevant to the pathogenesis of AD [14, 29, 66]. Alteration in endophilin 1, a synaptic vesicle protein, has been found to associate with AD pathology [67].

Synaptic dysfunction and synapse loss contribute importantly to cognitive deficits of AD [4–7]. Loss of synapses is one of the hallmarks of AD [68], and a better disease predictor than the amyloid plaque load [7]. As synaptic dysfunction begins early in the disease and is likely

reflected morphologically by synapse loss, the investigation of the link between synaptic function and cognitive decline has been extensively conducted in mouse models of AD or from post mortem human tissue samples [69–71]. Synaptic marker proteins, synaptophysin and PSD95, are essential components of synaptic structure and function [37]. Reduced expression of the synaptophysin, a presynaptic vesicle protein was reported in hippocampus and associated cortices of AD patients and was responsible for cognitive decline [7, 72, 73]. The density of synatophysin positive presynaptic terminals was reduced by ~30% in genetic human disease mice carrying mutant form of human AβPP and expression of human Aβ compared to nontransgenic mice at 2–3 months of age well before amyloid plaque formation [64]. Similarly, both mRNA and protein levels of postsynaptic protein PSD95 were markedly reduced in human AD-affected inferior temporal cortex of AD patients [74]. In corollary to this study, we demonstrated that the protein levels of synaptophysin and PSD95 were robustly lower in the differentiated AD cybrid cells compared to the differentiated non-AD cybrid cells, suggesting that reduction in expression of pre- and post-synaptic proteins, such as synaptophysin and PSD95, results in structural and functional alterations in synaptic maturation and development in AD cybrid cells upon abnormal neuronal differentiation. Owing to an essential energy-supplying organelles, mitochondria are particularly important to neuron metabolism, function, and neurotransmitter synthesis and transport [75]. Mitochondria distributed along neuronal dendrites actively participate in the morphogenesis and plasticity of spines and synapses [76–78]. Reduction in dendritic mitochondria leads to loss of synapses and number of dendritic spines, while increased dendritic mitochondrial content and mitochondrial activity improve plasticity of spines and synapses [78, 79]. Mounting evidence, including ours, has clearly demonstrated the early deficits in synaptic mitochondria in AD-affected brains, which correlate to synaptic loss [30, 80]. The effect of AD-associated mitochondrial defects on synaptogenesis remains to be determined. We previously demonstrated mitochondrial dysfunction in AD cybrids under “rest” or undifferentiated status [17]. Our recent study showed, after differentiation, AD cybrids demonstrated decreased mitochondrial function, lower mitochondrial membrane potential, deficits in AD mitochondrial transport, and significantly elevated mitochondrial oxidative stress along with a mal-differentiated status [22]. Moreover, the present study is to address whether AD-mediated mitochondrial dysfunction links to synaptic formation and maturation. In differentiated AD cybrids, synaptic loss was correlated to mitochondrial dysfunction and elevated mitochondrial oxidative stress. These findings are in agreement with those studies revealing the relationship between dendritic mitochondrial deficiency and synaptic loss in AD models. In view of the protective effect of antioxidant on mitochondrial function and ROS production/accumulation [14, 22, 31], increased mitochondrial oxidative could potentiate synaptic alterations. Indeed, our results show that abrogation of mitochondria ROS increases the formation of neurol process and the production of synaptic proteins in AD cybrid cells induced by SAT differentiation. The proper mitochondrial function are critical for mitochondrial dynamics by maintaining the balance of mitochondrial fission and fusion and synapse formation [17, 18, 81]. Excessive mitochondrial ROS causes imbalance of mitochondrial fission and fusion in mild cognitive impairment-and AD-affected mitochondria. The suppression of overproduction of ROS rescues abnormal dynamics and mitochondrial transport [17, 18, 22]. Thus, AD-mediated the disruption of mitochondrial dynamics and mitochondrial trafficking could also be the possible mechanism

underling impairment in synaptic development and maturation. It requires further investigation to uncover the link of the imbalance of mitochondrial fission and fusion to synaptogenesis insulted by AD-affected mitochondria in AD cybrid cells under differentiated status.

The p38 MAP kinases are a family of serine/threonine protein kinases and involved in cellular responses to external stress signals. Phosphorylation of p38 MAP kinase occurred in response to oxidative stress such as hypoxia [82] and H_2O_2 administered exogenously [83]. Accumulating evidence indicates that p38 MAP kinase plays a pivotal role in AD pathophysiology and its inhibitors offer benefits to AD patients [43, 84]. Higher levels of phosphorylated p38 were reported in AD cybrids [24, 38], however, the involvement of p38 in mitochondrial dysfunction and oxidative stress in AD remains unknown. The link of AD mitochondria-mediated activation of p38/ROS to synaptogenesis is poorly understood. By applying a recognized inhibitor of p38 MAP kinase, SB203580, we provide the direct evidence that activation of p38 MAP kinase signaling pathway contributes to mitochondrial dysfunction in differentiated AD cybrids. In addition, we demonstrated that inhibition of p38 MAP kinase activation significantly reduced mitochondrial and cellular ROS levels and improved mitochondrial function, resulting in normal differentiation and synaptic development in the differentiated AD cybrids. To clarify, Fig. 4 showed levels of phospho-p38 kinase in both AD and non-AD cybrid cells under a low concentration of staurosporine (10 nM)-induced differentiation. The phospho-p38 levels were significantly elevated by ~2.5 fold in AD cybrid cells compared to non-AD cybrid cells, suggesting AD-associated activation of p38 kinase in AD cybrid cells may not fully depend on staurosporine-induced p38 MAP kinase activation. These data suggest the role of p38 on AD mitochondrial defects and oxidative stress. However, whether other MAP kinase pathways, such as c-Jun N-terminal kinase (JNK) [85, 86] and extracellular signal-regulated protein (ERK) [18, 87], may also be involved in AD-mediated aberrant neuronal differentiation and synaptic formation.

In summary, we have demonstrated that AD mitochondrial defects contribute to synaptic deficiency in differentiated AD-cybrids. The mitochondrial dysfunction and abnormally elevated mitochondrial oxidative stress are responsible for the synaptic alteration through the activation of p38 MAP kinase signaling pathway. Importantly, blockade p38 MAP kinase activation by pharmaceutical inhibitor not only improves mitochondrial function and suppresses oxidative stress, but also restores the neuronal differentiation and the formation of synapses in cybrid cells containing AD mitochondria. Thus, modulating MAP kinase signaling pathway could be a therapeutical intervention in protection against early synaptic deficiency associated with memory loss and cognitive decline, and thereby defeating AD at an early stage. Furthermore, the outcomes of studying AD-derived mitochondria using human AD cybrid cells as an *ex-vivo* model, can be interpreted more meaningfully to the sporadic AD-specific mitochondrial defects because clinical data are available for the proposed AD cases, which significantly enhances our understanding of the AD pathogenesis and exploring the therapeutic strategy.

Supplementary Material

Refer to Web version on PubMed Central for supplementary material.

Acknowledgments

This study was supported by grants from the National Institute on Aging (R37AG037319, R01AG044793, R56AG053041), National institute of Neurological disorder and Stroke (R01NS 089116). We thank Dr. Swerdlow for providing cybrid cells for our study and Generation and characterization of cybrid cells were supported by the University of Kansas Alzheimer's Disease Center (NIA P30AG035982). We thank Justin T. Douglas for assistance in using EPR instrumentation. The EPR instrumentation was provided by NSF Chemical Instrumentation Grant (# 0946883).

Authors' disclosures available online (http://j-alz.com/manuscript-disclosures/17-0283r1).

References

1. Harris KM, Weinberg RJ. Ultrastructure of synapses in the mammalian brain. Cold Spring Harb Perspect Biol. 2012; 4 pii: a005587.
2. Mayford M, Siegelbaum SA, Kandel ER. Synapses and memory storage. Cold Spring Harb Perspect Biol. 2012; 4 pii: a005751.
3. Hardy J, Selkoe DJ. The amyloid hypothesis of Alzheimer's disease: Progress and problems on the road to therapeutics. Science. 2002; 297:353–356. [PubMed: 12130773]
4. DeKosky ST, Scheff SW. Synapse loss in frontal cortex biopsies in Alzheimer's disease: Correlation with cognitive severity. Ann Neurol. 1990; 27:457–464. [PubMed: 2360787]
5. Hamos JE, DeGennaro LJ, Drachman DA. Synaptic loss in Alzheimer's disease and other dementias. Neurology. 1989; 39:355–361. [PubMed: 2927643]
6. Robinson JL, Molina-Porcel L, Corrada MM, Raible K, Lee EB, Lee VM, Kawas CH, Trojanowski JQ. Perforant path synaptic loss correlates with cognitive impairment and Alzheimer's disease in the oldest-old. Brain. 2014; 137:2578–2587. [PubMed: 25012223]
7. Terry RD, Masliah E, Salmon DP, Butters N, DeTeresa R, Hill R, Hansen LA, Katzman R. Physical basis of cognitive alterations in Alzheimer's disease: Synapse loss is the major correlate of cognitive impairment. Ann Neurol. 1991; 30:572–580. [PubMed: 1789684]
8. Parihar MS, Brewer GJ. Amyloid-beta as a modulator of synaptic plasticity. J Alzheimers Dis. 2010; 22:741–763. [PubMed: 20847424]
9. Gylys KH, Fein JA, Yang F, Wiley DJ, Miller CA, Cole GM. Synaptic changes in Alzheimer's disease: Increased amyloid-beta and gliosis in surviving terminals is accompanied by decreased PSD-95 fluorescence. Am J Pathol. 2004; 165:1809–1817. [PubMed: 15509549]
10. Arendt T. Synaptic degeneration in Alzheimer's disease. Acta Neuropathol. 2009; 118:167–179. [PubMed: 19390859]
11. Reddy PH, Tripathi R, Troung Q, Tirumala K, Reddy TP, Anekonda V, Shirendeb UP, Calkins MJ, Reddy AP, Mao P, Manczak M. Abnormal mitochondrial dynamics and synaptic degeneration as early events in Alzheimer's disease: Implications to mitochondria-targeted antioxidant therapeutics. Biochim Biophys Acta. 2012; 1822:639–649. [PubMed: 22037588]
12. Tampellini D, Capetillo-Zarate E, Dumont M, Huang Z, Yu F, Lin MT, Gouras GK. Effects of synaptic modulation on beta-amyloid, synaptophysin, and memory performance in Alzheimer's disease transgenic mice. J Neurosci. 2010; 30:14299–14304. [PubMed: 20980585]
13. Hauptmann S, Scherping I, Drose S, Brandt U, Schulz KL, Jendrach M, Leuner K, Eckert A, Muller WE. Mitochondrial dysfunction: An early event in Alzheimer pathology accumulates with age in AD transgenic mice. Neurobiol Aging. 2009; 30:1574–1586. [PubMed: 18295378]
14. Fang D, Wang Y, Zhang Z, Du H, Yan S, Sun Q, Zhong C, Wu L, Vangavaragu JR, Yan S, Hu G, Guo L, Rabinowitz M, Glaser E, Arancio O, Sosunov AA, McKhann GM, Chen JX, Yan SS. Increased neuronal PreP activity reduces Abeta accumulation, attenuates neuroinflammation and improves mitochondrial and synaptic function in Alzheimer disease's mouse model. Hum Mol Genet. 2015; 24:5198–5210. [PubMed: 26123488]

15. Yao J, Du H, Yan S, Fang F, Wang C, Lue LF, Guo L, Chen D, Stern DM, Gunn Moore FJ, Xi Chen J, Arancio O, Yan SS. Inhibition of amyloid-beta (Abeta) peptide-binding alcohol dehydrogenase-Abeta interaction reduces Abeta accumulation and improves mitochondrial function in a mouse model of Alzheimer's disease. J Neurosci. 2011; 31:2313–2320. [PubMed: 21307267]
16. King MP, Attardi G. Human cells lacking mtDNA: Repopulation with exogenous mitochondria by complementation. Science. 1989; 246:500–503. [PubMed: 2814477]
17. Gan X, Huang S, Wu L, Wang Y, Hu G, Li G, Zhang H, Yu H, Swerdlow RH, Chen JX, Yan SS. Inhibition of ERK-DLP1 signaling and mitochondrial division alleviates mitochondrial dysfunction in Alzheimer's disease cybrid cell. Biochim Biophys Acta. 2014; 1842:220–231. [PubMed: 24252614]
18. Gan X, Wu L, Huang S, Zhong C, Shi H, Li G, Yu H, Howard Swerdlow R, Xi Chen J, Yan SS. Oxidative stress-mediated activation of extracellular signal-regulated kinase contributes to mild cognitive impairment-related mitochondrial dysfunction. Free Radic Biol Med. 2014; 75:230–240. [PubMed: 25064321]
19. Trimmer PA, Borland MK. Differentiated Alzheimer's disease transmitochondrial cybrid cell lines exhibit reduced organelle movement. Antioxid Redox Signal. 2005; 7:1101–1109. [PubMed: 16115014]
20. Trimmer PA, Swerdlow RH, Parks JK, Keeney P, Bennett JP Jr, Miller SW, Davis RE, Parker WD Jr. Abnormal mitochondrial morphology in sporadic Parkinson's and Alzheimer's disease cybrid cell lines. Exp Neurol. 2000; 162:37–50. [PubMed: 10716887]
21. Cardoso SM, Santana I, Swerdlow RH, Oliveira CR. Mitochondria dysfunction of Alzheimer's disease cybrids enhances Abeta toxicity. J Neurochem. 2004; 89:1417–1426. [PubMed: 15189344]
22. Yu Q, Fang D, Swerdlow RH, Yu H, Chen JX, Yan SS. Antioxidants rescue mitochondrial transport in differentiated Alzheimer's disease transmitochondrial cybrid cells. J Alzheimers Dis. 2016; 54:679–690. [PubMed: 27567872]
23. Silva DF, Santana I, Esteves AR, Baldeiras I, Arduino DM, Oliveira CR, Cardoso SM. Prodromal metabolic phenotype in MCI cybrids: Implications for Alzheimer's disease. Curr Alzheimer Res. 2013; 10:180–190. [PubMed: 22746213]
24. Silva DF, Selfridge JE, Lu J, EL, Roy N, Hutfles L, Burns JM, Michaelis EK, Yan S, Cardoso SM, Swerdlow RH. Bioenergetic flux, mitochondrial mass and mitochondrial morphology dynamics in AD and MCI cybrid cell lines. Hum Mol Genet. 2013; 22:3931–3946. [PubMed: 23740939]
25. Albert MS, DeKosky ST, Dickson D, Dubois B, Feldman HH, Fox NC, Gamst A, Holtzman DM, Jagust WJ, Petersen RC, Snyder PJ, Carrillo MC, Thies B, Phelps CH. The diagnosis of mild cognitive impairment due to Alzheimer's disease: Recommendations from the National Institute on Aging-Alzheimer's Association workgroups on diagnostic guidelines for Alzheimer's disease. Alzheimers Dement. 2011; 7:270–279. [PubMed: 21514249]
26. Miller SW, Trimmer PA, Parker WD Jr, Davis RE. Creation and characterization of mitochondrial DNA-depleted cell lines with "neuronal-like" properties. J Neurochem. 1996; 67:1897–1907. [PubMed: 8863494]
27. Swerdlow RH. Mitochondria and cell bioenergetics: Increasingly recognized components and a possible etiologic cause of Alzheimer's disease. Antioxid Redox Signal. 2012; 16:1434–1455. [PubMed: 21902597]
28. Swerdlow RH. Mitochondria in cybrids containing mtDNA from persons with mitochondriopathies. J Neurosci Res. 2007; 85:3416–3428. [PubMed: 17243174]
29. Du H, Guo L, Fang F, Chen D, Sosunov AA, McKhann GM, Yan Y, Wang C, Zhang H, Molkentin JD, Gunn-Moore FJ, Vonsattel JP, Arancio O, Chen JX, Yan SD. Cyclophilin D deficiency attenuates mitochondrial and neuronal perturbation and ameliorates learning and memory in Alzheimer's disease. Nat Med. 2008; 14:1097–1105. [PubMed: 18806802]
30. Du H, Guo L, Yan S, Sosunov AA, McKhann GM, Yan SS. Early deficits in synaptic mitochondria in an Alzheimer's disease mouse model. Proc Natl Acad Sci U S A. 2010; 107:18670–18675. [PubMed: 20937894]

31. Fang D, Zhang Z, Li H, Yu Q, Douglas JT, Bratasz A, Kuppusamy P, Yan SS. Increased electron paramagnetic resonance signal correlates with mitochondrial dysfunction and oxidative stress in an Alzheimer's disease mouse brain. J Alzheimers Dis. 2016; 51:571–580. [PubMed: 26890765]
32. Prince JA, Oreland L. Staurosporine differentiated human SH-SY5Y neuroblastoma cultures exhibit transient apoptosis and trophic factor independence. Brain Res Bull. 1997; 43:515–523. [PubMed: 9254022]
33. Trimmer PA, Schwartz KM, Borland MK, De Taboada L, Streeter J, Oron U. Reduced axonal transport in Parkinson's disease cybrid neurites is restored by light therapy. Mol Neurodegener. 2009; 4:26. [PubMed: 19534794]
34. Borland MK, Trimmer PA, Rubinstein JD, Keeney PM, Mohanakumar K, Liu L, Bennett JP Jr. Chronic, low-dose rotenone reproduces Lewy neurites found in early stages of Parkinson's disease, reduces mitochondrial movement and slowly kills differentiated SH-SY5Y neural cells. Mol Neurodegener. 2008; 3:21. [PubMed: 19114014]
35. Soltani MH, Pichardo R, Song Z, Sangha N, Camacho F, Satyamoorthy K, Sangueza OP, Setaluri V. Microtubule-associated protein 2, a marker of neuronal differentiation, induces mitotic defects, inhibits growth of melanoma cells, and predicts metastatic potential of cutaneous melanoma. Am J Pathol. 2005; 166:1841–1850. [PubMed: 15920168]
36. Sarnat HB, Nochlin D, Born DE. Neuronal nuclear antigen (NeuN): A marker of neuronal maturation in early human fetal nervous system. Brain Dev. 1998; 20:88–94. [PubMed: 9545178]
37. Cohen-Cory S. The developing synapse: Construction and modulation of synaptic structures and circuits. Science. 2002; 298:770–776. [PubMed: 12399577]
38. Zhang H, Liu Y, Lao M, Ma Z, Yi X. Puerarin protects Alzheimer's disease neuronal cybrids from oxidant-stress induced apoptosis by inhibiting pro-death signaling pathways. Exp Gerontol. 2011; 46:30–37. [PubMed: 20933077]
39. Guo L, Du H, Yan S, Wu X, McKhann GM, Chen JX, Yan SS. Cyclophilin D deficiency rescues axonal mitochondrial transport in Alzheimer's neurons. PLoS One. 2013; 8:e54914. [PubMed: 23382999]
40. Alikhani N, Guo L, Yan S, Du H, Pinho CM, Chen JX, Glaser E, Yan SS. Decreased proteolytic activity of the mitochondrial amyloid-beta degrading enzyme, PreP peptidasome, in Alzheimer's disease brain mitochondria. J Alzheimers Dis. 2011; 27:75–87. [PubMed: 21750375]
41. Lustbader JW, Cirilli M, Lin C, Xu HW, Takuma K, Wang N, Caspersen C, Chen X, Pollak S, Chaney M, Trinchese F, Liu S, Gunn-Moore F, Lue LF, Walker DG, Kuppusamy P, Zewier ZL, Arancio O, Stern D, Yan SS, Wu H. ABAD directly links Abeta to mitochondrial toxicity in Alzheimer's disease. Science. 2004; 304:448–452. [PubMed: 15087549]
42. Takuma K, Fang F, Zhang W, Yan S, Fukuzaki E, Du H, Sosunov A, McKhann G, Funatsu Y, Nakamichi N, Nagai T, Mizoguchi H, Ibi D, Hori O, Ogawa S, Stern DM, Yamada K, Yan SS. RAGE-mediated signaling contributes to intraneuronal transport of amyloid-beta and neuronal dysfunction. Proc Natl Acad Sci U S A. 2009; 106:20021–20026. [PubMed: 19901339]
43. Arancio O, Zhang HP, Chen X, Lin C, Trinchese F, Puzzo D, Liu S, Hegde A, Yan SF, Stern A, Luddy JS, Lue LF, Walker DG, Roher A, Buttini M, Mucke L, Li W, Schmidt AM, Kindy M, Hyslop PA, Stern DM, Du Yan SS. RAGE potentiates Abeta-induced perturbation of neuronal function in transgenic mice. EMBO J. 2004; 23:4096–4105. [PubMed: 15457210]
44. Santabarbara-Ruiz P, Lopez-Santillan M, Martinez-Rodriguez I, Binagui-Casas A, Perez L, Milan M, Corominas M, Serras F. ROS-induced JNK and p38 signaling is required for unpaired cytokine activation during Drosophila regeneration. PLoS Genet. 2015; 11:e1005595. [PubMed: 26496642]
45. Matsuyama D, Kawahara K. Oxidative stress-induced formation of a positive-feedback loop for the sustained activation of p38 MAPK leading to the loss of cell division in cardiomyocytes soon after birth. Basic Res Cardiol. 2011; 106:815–828. [PubMed: 21479589]
46. Lee MW, Park SC, Yang YG, Yim SO, Chae HS, Bach JH, Lee HJ, Kim KY, Lee WB, Kim SS. The involvement of reactive oxygen species (ROS) and p38 mitogen-activated protein (MAP) kinase in TRAIL/Apo2L-induced apoptosis. FEBS Lett. 2002; 512:313–318. [PubMed: 11852102]
47. Origlia N, Arancio O, Domenici L, Yan SS. MAPK, beta-amyloid and synaptic dysfunction: The role of RAGE. Expert Rev Neurother. 2009; 9:1635–1645. [PubMed: 19903023]

48. Origlia N, Bonadonna C, Rosellini A, Leznik E, Arancio O, Yan SS, Domenici L. Microglial receptor for advanced glycation end product-dependent signal pathway drives beta-amyloid-induced synaptic depression and long-term depression impairment in entorhinal cortex. J Neurosci. 2010; 30:11414–11425. [PubMed: 20739563]

49. Origlia N, Criscuolo C, Arancio O, Yan SS, Domenici L. RAGE inhibition in microglia prevents ischemia-dependent synaptic dysfunction in an amyloid-enriched environment. J Neurosci. 2014; 34:8749–8760. [PubMed: 24966375]

50. Borodkina A, Shatrova A, Abushik P, Nikolsky N, Burova E. Interaction between ROS dependent DNA damage, mitochondria and p38 MAPK underlies senescence of human adult stem cells. Aging (Albany NY). 2014; 6:481–495. [PubMed: 24934860]

51. Huang S, Wang Y, Gan X, Fang D, Zhong C, Wu L, Hu G, Sosunov AA, McKhann GM, Yu H, Yan SS. Drp1-mediated mitochondrial abnormalities link to synaptic injury in diabetes model. Diabetes. 2015; 64:1728–1742. [PubMed: 25412623]

52. Zhang Z, Wang Y, Yan S, Du F, Yan SS. NR2B-dependent cyclophilin D translocation suppresses the recovery of synaptic transmission after oxygen-glucose deprivation. Biochim Biophys Acta. 2015; 1852:2225–2234. [PubMed: 26232180]

53. Wang Y, Wu L, Fang D, Zhong C, Chen JX, Yan SS. Synergistic exacerbation of mitochondrial and synaptic dysfunction and resultant learning and memory deficit in a mouse model of diabetic Alzheimer's disease. J Alzheimers Dis. 2014; 43:451–463.

54. Du H, Guo L, Wu X, Sosunov AA, McKhann GM, Chen JX, Yan SS. Cyclophilin D deficiency rescues Abeta-impaired PKA/CREB signaling and alleviates synaptic degeneration. Biochim Biophys Acta. 2014; 1842:2517–2527. [PubMed: 23507145]

55. Du H, Guo L, Zhang W, Rydzewska M, Yan S. Cyclophilin D deficiency improves mitochondrial function and learning/memory in aging Alzheimer disease mouse model. Neurobiol Aging. 2011; 32:398–406. [PubMed: 19362755]

56. Constantinescu R, Constantinescu AT, Reichmann H, Janetzky B. Neuronal differentiation and long-term culture of the human neuroblastoma line SH-SY5Y. J Neural Transm. 2007; (Suppl 72): 17–28.

57. Encinas M, Iglesias M, Liu Y, Wang H, Muhaisen A, Cena V, Gallego C, Comella JX. Sequential treatment of SH-SY5Y cells with retinoic acid and brain-derived neurotrophic factor gives rise to fully differentiated, neurotrophic factor-dependent, human neuron-like cells. J Neurochem. 2000; 75:991–1003. [PubMed: 10936180]

58. Regulska M, Leskiewicz M, Budziszewska B, Kutner A, Jantas D, Basta-Kaim A, Kubera M, Jaworska-Feil L, Lason W. Inhibitory effects of 1,25-dihydroxyvitamin D3 and its low-calcemic analogues on staurosporine-induced apoptosis. Pharmacol Rep. 2007; 59:393–401. [PubMed: 17901567]

59. Mikami M, Goubaeva F, Song JH, Lee HT, Yang J. beta-Adrenoceptor blockers protect against staurosporine-induced apoptosis in SH-SY5Y neuroblastoma cells. Eur J Pharmacol. 2008; 589:14–21. [PubMed: 18534571]

60. McNeill-Blue C, Wetmore BA, Sanchez JF, Freed WJ, Merrick BA. Apoptosis mediated by p53 in rat neural AF5 cells following treatment with hydrogen peroxide and staurosporine. Brain Res. 2006; 1112:1–15. [PubMed: 16901471]

61. Yang XP, Liu TY, Qin XY, Yu LC. Potential protection of 2,3,5,4′-tetrahydroxystilbene-2-O-beta-D-glucoside against staurosporine-induced toxicity on cultured rat hippocampus neurons. Neurosci Lett. 2014; 576:79–83. [PubMed: 24887581]

62. Wu SN, Wang YJ, Lin MW. Potent stimulation of large-conductance Ca2+-activated K+ channels by rottlerin, an inhibitor of protein kinase C-delta, in pituitary tumor (GH3) cells and in cortical neuronal (HCN-1A) cells. J Cell Physiol. 2007; 210:655–666. [PubMed: 17133362]

63. Shafit-Zagardo B, Kalcheva N. Making sense of the multiple MAP-2 transcripts and their role in the neuron. Mol Neurobiol. 1998; 16:149–162. [PubMed: 9588626]

64. Hsia AY, Masliah E, McConlogue L, Yu GQ, Tatsuno G, Hu K, Kholodenko D, Malenka RC, Nicoll RA, Mucke L. Plaque-independent disruption of neural circuits in Alzheimer's disease mouse models. Proc Natl Acad Sci U S A. 1999; 96:3228–3233. [PubMed: 10077666]

65. Mullen RJ, Buck CR, Smith AM. NeuN, a neuronal specific nuclear protein in vertebrates. Development. 1992; 116:201–211. [PubMed: 1483388]

66. Kamat PK, Kalani A, Rai S, Swarnkar S, Tota S, Nath C, Tyagi N. Mechanism of oxidative stress and synapse dysfunction in the pathogenesis of Alzheimer's disease: Understanding the therapeutics strategies. Mol Neurobiol. 2016; 53:648–661. [PubMed: 25511446]

67. Ren Y, Xu HW, Davey F, Taylor M, Aiton J, Coote P, Fang F, Yao J, Chen D, Chen JX, Yan SD, Gunn-Moore FJ. Endophilin I expression is increased in the brains of Alzheimer disease patients. J Biol Chem. 2008; 283:5685–5691. [PubMed: 18167351]

68. Pozueta J, Lefort R, Shelanski ML. Synaptic changes in Alzheimer's disease and its models. Neuroscience. 2013; 251:51–65. [PubMed: 22687952]

69. Arnold SE, Louneva N, Cao K, Wang LS, Han LY, Wolk DA, Negash S, Leurgans SE, Schneider JA, Buchman AS, Wilson RS, Bennett DA. Cellular, synaptic, and biochemical features of resilient cognition in Alzheimer's disease. Neurobiol Aging. 2013; 34:157–168. [PubMed: 22554416]

70. Chakroborty S, Stutzmann GE. Early calcium dysregulation in Alzheimer's disease: Setting the stage for synaptic dysfunction. Sci China Life Sci. 2011; 54:752–762. [PubMed: 21786198]

71. Edmonds EC, Delano-Wood L, Galasko DR, Salmon DP, Bondi MW. Subtle cognitive decline and biomarker staging in preclinical Alzheimer's disease. J Alzheimers Dis. 2015; 47:231–242. [PubMed: 26402771]

72. Sze CI, Troncoso JC, Kawas C, Mouton P, Price DL, Martin LJ. Loss of the presynaptic vesicle protein synaptophysin in hippocampus correlates with cognitive decline in Alzheimer disease. J Neuropathol Exp Neurol. 1997; 56:933–944. [PubMed: 9258263]

73. Dickson DW, Crystal HA, Bevona C, Honer W, Vincent I, Davies P. Correlations of synaptic and pathological markers with cognition of the elderly. Neurobiol Aging. 1995; 16:285–298. discussion 298–304. [PubMed: 7566338]

74. Proctor DT, Coulson EJ, Dodd PR. Reduction in post-synaptic scaffolding PSD-95 and SAP-102 protein levels in the Alzheimer inferior temporal cortex is correlated with disease pathology. J Alzheimers Dis. 2010; 21:795–811. [PubMed: 20634587]

75. Chan DC. Mitochondria: Dynamic organelles in disease, aging, and development. Cell. 2006; 125:1241–1252. [PubMed: 16814712]

76. Hollenbeck PJ. The pattern and mechanism of mitochondrial transport in axons. Front Biosci. 1996; 1:d91–102. [PubMed: 9159217]

77. Kann O, Kovacs R. Mitochondria and neuronal activity. Am J Physiol Cell Physiol. 2007; 292:C641–C657. [PubMed: 17092996]

78. Li Z, Okamoto K, Hayashi Y, Sheng M. The importance of dendritic mitochondria in the morphogenesis and plasticity of spines and synapses. Cell. 2004; 119:873–887. [PubMed: 15607982]

79. Tada T, Sheng M. Molecular mechanisms of dendritic spine morphogenesis. Curr Opin Neurobiol. 2006; 16:95–101. [PubMed: 16361095]

80. Calkins MJ, Manczak M, Mao P, Shirendeb U, Reddy PH. Impaired mitochondrial biogenesis, defective axonal transport of mitochondria, abnormal mitochondrial dynamics and synaptic degeneration in a mouse model of Alzheimer's disease. Hum Mol Genet. 2011; 20:4515–4529. [PubMed: 21873260]

81. Fang D, Yan S, Yu Q, Chen D, Yan SS. Mfn2 is required for mitochondrial development and synapse formation in human induced pluripotent stem cells/hiPSC derived cortical neurons. Sci Rep. 2016; 6:31462. [PubMed: 27535796]

82. Kulisz A, Chen N, Chandel NS, Shao Z, Schumacker PT. Mitochondrial ROS initiate phosphorylation of p38 MAP kinase during hypoxia in cardiomyocytes. Am J Physiol Lung Cell Mol Physiol. 2002; 282:L1324–L1329. [PubMed: 12003789]

83. Aggeli IK, Gaitanaki C, Beis I. Involvement of JNKs and p38-MAPK/MSK1 pathways in H2O2-induced upregulation of heme oxygenase-1 mRNA in H9c2 cells. Cell Signal. 2006; 18:1801–1812. [PubMed: 16531007]

84. Munoz L, Ammit AJ. Targeting p38 MAPK pathway for the treatment of Alzheimer's disease. Neuropharmacology. 2010; 58:561–568. [PubMed: 19951717]

85. Atzori C, Ghetti B, Piva R, Srinivasan AN, Zolo P, Delisle MB, Mirra SS, Migheli A. Activation of the JNK/p38 pathway occurs in diseases characterized by tau protein pathology and is related to tau phosphorylation but not to apoptosis. J Neuropathol Exp Neurol. 2001; 60:1190–1197. [PubMed: 11764091]

86. Okazawa H, Estus S. The JNK/c-Jun cascade and Alzheimer's disease. Am J Alzheimers Dis Other Demen. 2002; 17:79–88. [PubMed: 11954673]

87. Kins S, Kurosinski P, Nitsch RM, Gotz J. Activation of the ERK and JNK signaling pathways caused by neuron-specific inhibition of PP2A in transgenic mice. Am J Pathol. 2003; 163:833–843. [PubMed: 12937125]

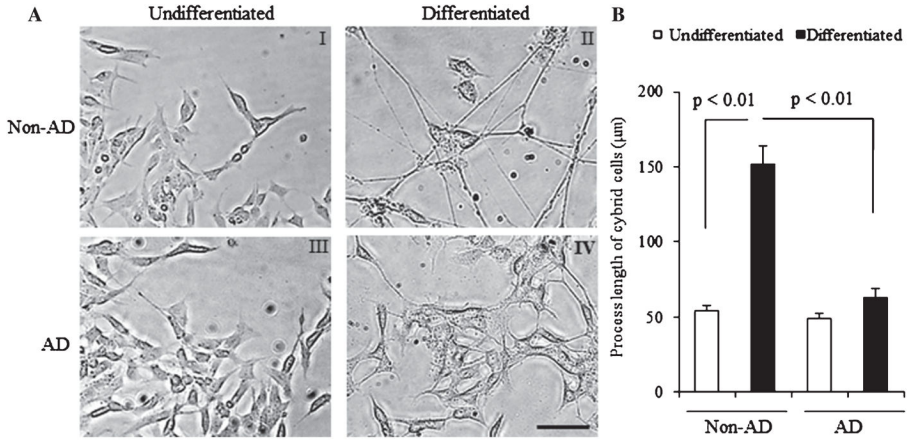

Fig. 1.

Comparison of differentiation status in neuronal processes between non-AD and AD cybrid cells during differentiation. A) Representative morphological images from non-AD and AD cybrid cells under undifferentiated conditions or induced by SAT (14 days after 10 nM staurosporine [SAT] treatment). Scale bar = 50 μm. B) Quantification of neuronal process length of cybrid cells using the image J program. Black bars denote the process length of cybrid cells following SAT treatment in both non-AD and AD groups. Open bars represent process lengths of undifferentiated cybrid cells without SAT treatment.

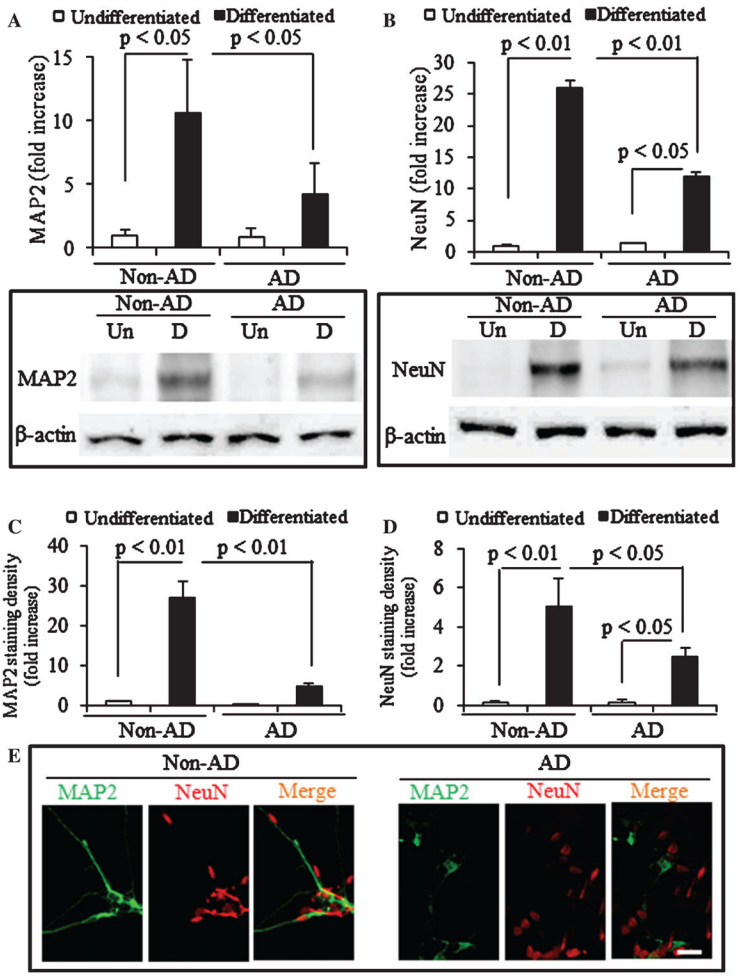

Fig. 2.

Expression of neuronal markers in non-AD and AD cybrid cells during differentiation. Immunoblotting of protein extracts from non-AD and AD cybrid cells for MAP2 (A) and NeuN (B) in the indicated groups of cells. β-actin was used for protein loading control. The upper panel displays quantification of immunoreactive bands for the corresponding protein relative to β-actin. Data are expressed as fold increase relative to undifferenciated non-AD cybrid cells. Quantification of fluorescent intensity of MAP2 (C) and NeuN (D), and (E), representative images of immunofluorescent staining for MAP2 (green) and NeuN (red) in the indicated groups of cybrid cells. Scale bar = 50 μm.

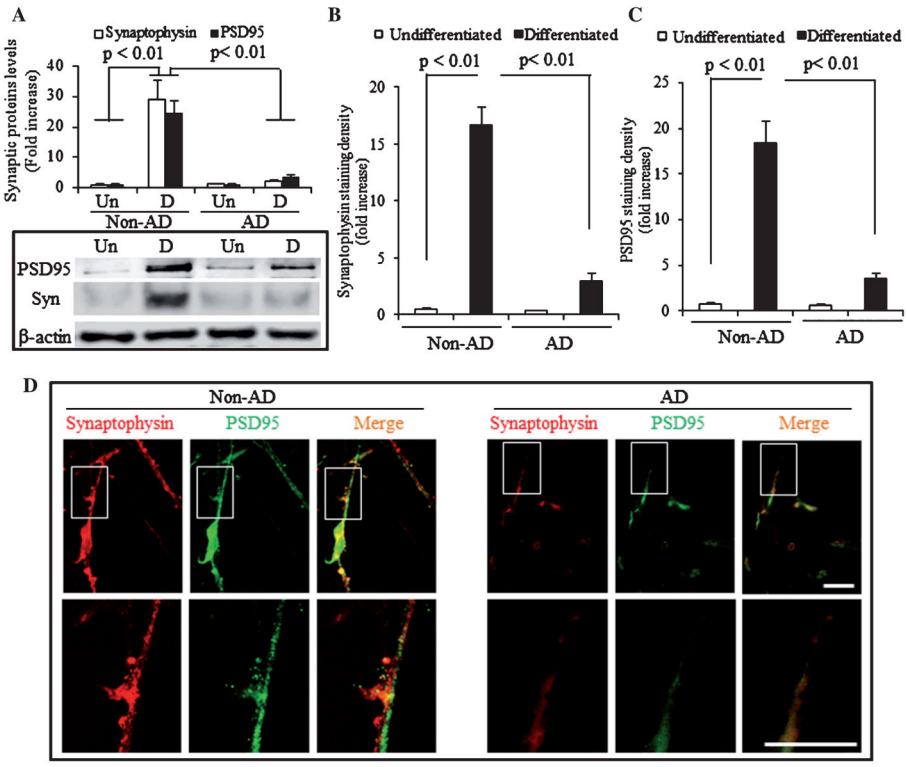

Fig. 3.

Expression of synaptic proteins in AD cybrid cells during differentiation. A) Immunoblotting of protein extracts from non-AD and AD cybrid cells for PSD95 and synaptophysin in the indicated groups of cells. β-actin was used for protein loading control. The upper panel displays quantification of immunoreactive bands for the corresponding protein relative to β-actin. Data are expressed as fold increase relative to undifferentiated non-AD cybrid cells. Quantification of fluorescent intensity of synaptophysin (B) and PSD95 (C). Representative images of immunofluorescent staining for synaptophysin (red) and PSD95 (green) in the indicated groups of cybrid cells (D). Scale bars = 50 μm.

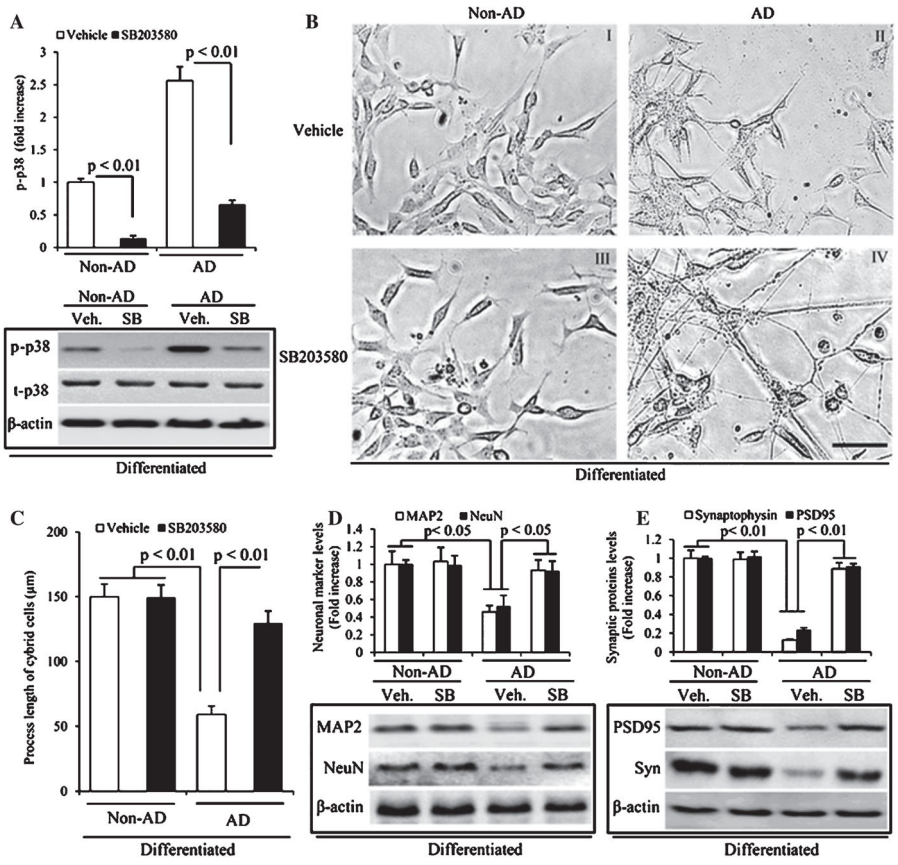

Fig. 4.

Effect of p38 signaling pathway and its inhibitor on neuronal differentiation and expression of synaptic proteins in AD cybrid cells during differentiation. A) Immunoblotting of protein extracts from non-AD and AD cybrid cells for p-p38 and t-p-38 in the indicated groups of cells. β-actin was used for protein loading control. The upper panel displays quantification of immunoreactive bands for the corresponding protein relative to β-actin. Data are expressed as fold increase relative to non-AD vehicle cybrid cells. Open bars represent the protein expression level of p-p38 in the indicated groups of cybrid cells without any treatment. Black bars denote the protein expression level of p-p38 in the indicated groups of cybrid cells with the treatment of SB203580. Scale bar = 50 μm. B) Representative morphological images of mitochondria in the processes of above differentiated non-AD and AD cybrid cells (I–IV). I and II: non-AD and AD cells under differentiation without any treatment. III and IV: non-AD and AD cybrid cells under differentiation with the addition of the inhibitor of P38, SB203580. C) Quantification of neuronal process length of cybrid cells using the image J program. D) Immunoblotting of protein extracts from differentiated non-AD and AD cybrid cells with or without SB203580 treatment for MAP2 and NeuN. β-actin was used for protein loading control. The upper panel displays quantification of immunoreactive bands for the corresponding protein relative to β-actin. Data are expressed as fold increase relative to non-AD vehicle cybrid cells. Open bars represent the protein expression level of MAP2 in the indicated groups of cybrid cells. Black bars denote the protein expression level of NeuN in the indicated groups of cybrid cells. E) Immunoblotting

of protein extracts from differentiated non-AD and AD cybrid cells with or without SB203580 treatment for PSD95 and Synaptophysin. β-actin was used for protein loading control. The upper panel displays quantification of immunoreactive bands for the corresponding protein relative to β-actin. Data are expressed as fold increase relative to non-AD vehicle cybrid cells.

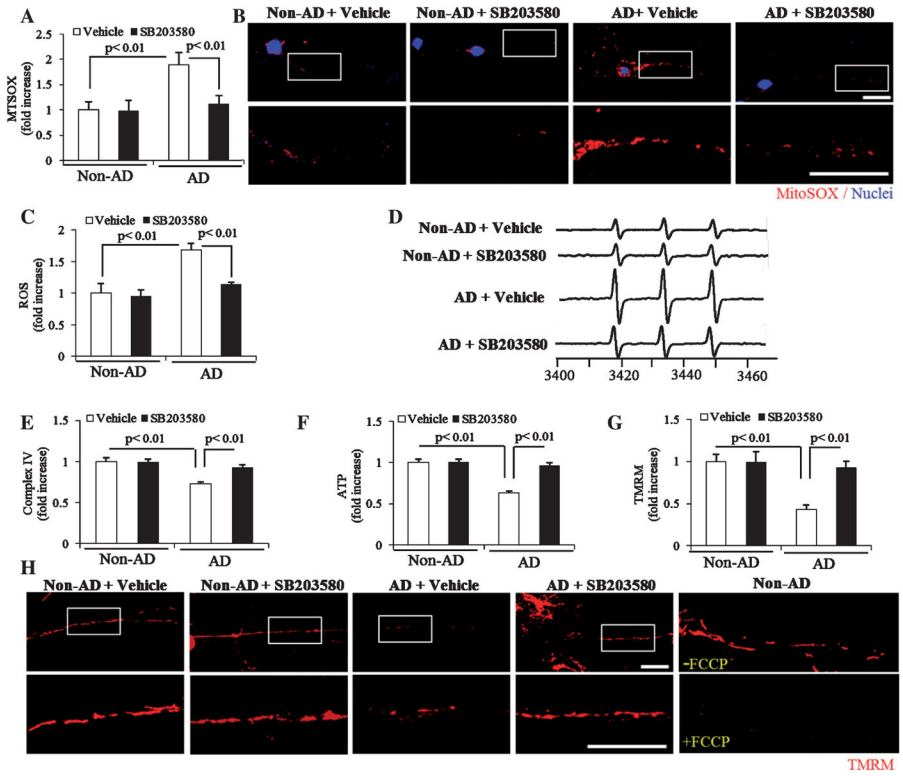

Fig. 5.

Effect of p38 MAP kinase pathway and its inhibitor on mitochondrial function and ROS in AD cybrid cells during differentiation. Mitochondrial ROS levels were measured by MitoSox staining intensity (A and B) and generation of ROS in the indicated groups of cells was detected by electron paramagnetic resonance (EPR) spectra (C–D). Enzymatic activity of complex IV (E), and cellular ATP levels (F) were determined in cell lysates from differentiated AD cybrid cells with or without the addition of SB203580. Data were expressed as fold increase relative to AD cybrid cells without the addition of SB203580 (vehicle treatment). Mitochondrial membrane potential was measured by TMRM staining intensity (G and H). Quantifications of immunofluorescent intensity for MitoSox (A), the signal intensity of EPR (C), and TMRM (G) in mitochondria of the indicated cybrid cells. The representative EPR and staining images were shown for EPR (D), and red fluorescence for Mitosox (B) and TMRM (H). Data were collected from 20–25 processes of each AD cybrid cell line with different treatments. Scale bars = 25 μm.

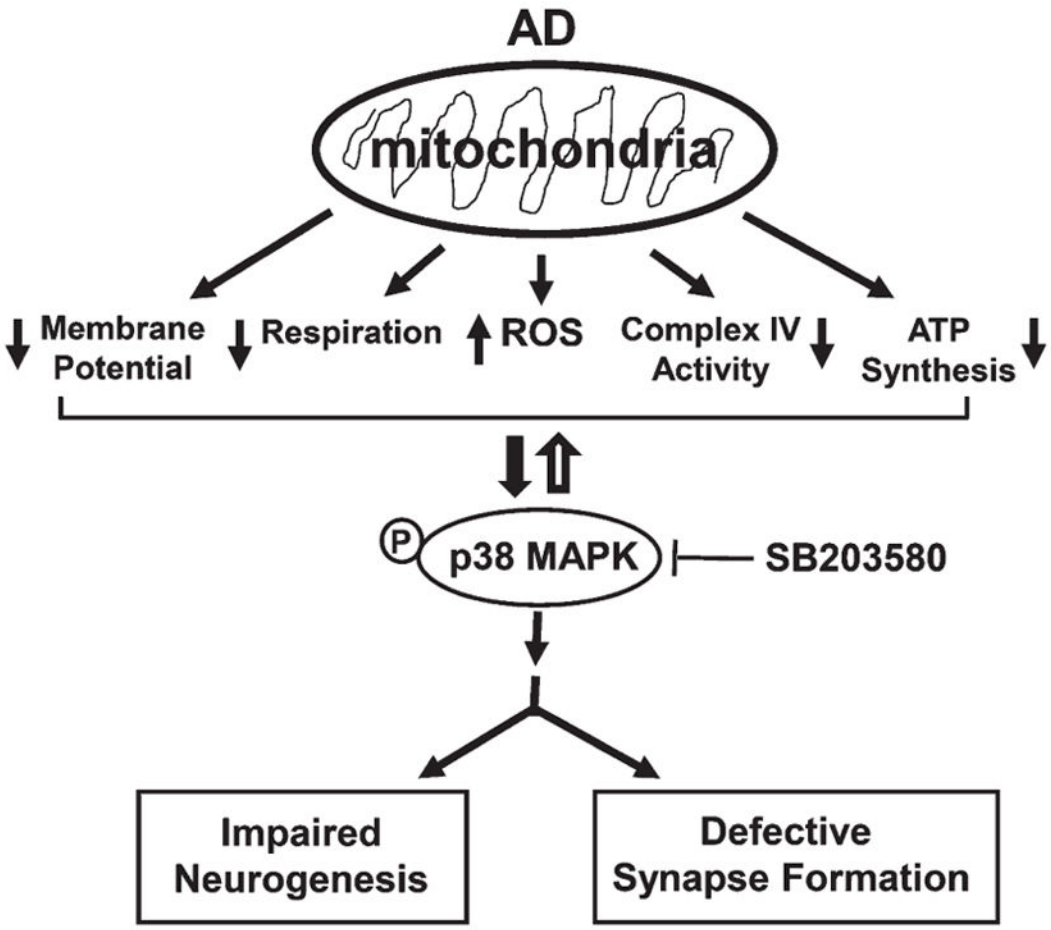

Fig. 6.

Schematic depiction of p38 MAP kinase pathway in response to elevated ROS levels and mitochondrial dysfunction, leading to arrested differentiation and synaptic deficits in AD cybrid cells. Meanwhile, activated p38 MAP kinase pathway in turn promotes ROS production and augments mitochondrial dysfunction, eventually exacerbates the impaired differentiation and synaptic deficits in AD cybrid cells. Thus, blocking p38 MAPK activation using a pharmacological inhibitor of p38 MAPK (SB203580) could reverses AD mitochondria-mediated detrimental effects by suppressing ROS production and accumulation, powering mitochondrial function, and maintaining normal differentiation and synaptic development.